3D Tomography using Efficient Wavefront Picking of Traveltimes

Abdullah AlTheyab

ABSTRACT

To reduce human labor in picking traveltimes in 3D data, first-arrivals are picked geographically on coarsely-sampled time-slices of the recorded shot gathers. Traveltime picks are interpolated in real-time in the polar coordinates to minimize the number of picks needed to track curved wavefronts. The picked first-arrival traveltimes are used in ray tomography to form an initial model for FWI. Results indicate an 80% reduction in human picking time compared to standard picking in the shot gather or common offset domains.

INTRODUCTION

Full-wavefield inversion methods such as full-waveform inversion (FWI) (Tarantola, 1984; Virieux and Operto, 2009) and differential-semblence optimization (DSO) (Symes and Carazzone, 1991), require a good initial velocity model to (1) avoid cycle-skipping issues (for FWI) and (2) minimize the number of computationally-intensive iterations. Inverting first-arrival traveltimes is the traditional method for generating accurate starting models (Woodward et al., 2008).

As the seismic industry moves toward denser source and receiver coverage per square area, high density data is becoming a heavy burden for visualization and picking of early arrivals for tomography, especially in the presence of irregularities in the acquisition geometry and complex geology. Tremendous human interaction is needed for Quality Control (QC), even when a robust automatic picking tool is available.

If the output of tomography is an initial model for full-waveform inversion, we propose a method for minimizing the amount of work needed for picking first breaks and QC-ing the picks. In this method, first-arrival wavefronts at sparse time-slices of a shot gather are picked on a map view. To avoid cycle-skipping, time-slice intervals are selected to be half the period of the minimum frequency that will be used in FWI. Every pick is characterized by azimuth and radial distance from the source along the surface. Traveltimes between picks are interpolated in polar coordinates to minimize the number of picks needed to represent curved wavefronts. Then, the picks are used as input to ray tomographic inversion to provide an initial model for FWI.

The method is applied to ocean bottom seismic (OBS) data from the GOM, and the results illustrate the potential of the method. The acquisition parameters are as follows:

- 234 OBS stations, spaced 400 meters apart in a 26 by 9 grid with varying depths with an average of 45 meters.
- 124 sail-lines with 50 meters spacing; each sail-line covers 18 km of distance with a shot spacing of 50 meters.

The data contain low-frequencies as low as 2 Hz with a minimum reliable frequency of 4 Hz. To avoid working with large number of shot gathers with a low number of receivers, we use reciprocity to convert common receiver gathers (CRG) to common shot gathers (CSG). Throughout this paper, we use CRG s for traveltime picking and for traveltime tomography.

METHODOLOGY

The key idea is to pick first-arrival traveltimes from time-slices of recorded CRGs instead of picking traveltimes from trace-to-trace. Time-slices do not have to be regular, but the wave-sampling has to be dense enough to be able to pick events on a map view. Conventional picking in common-shot gathers and common-offset gathers is difficult to coordinate in order to assure areal consistency of picks. In addition, generating the common-offset or common-azimuth gathers for irregular 3D datasets is

0

not trivial and require additional steps of regularization. Areal displays of wavefronts, on the other hand, are more easily evaluated for picking of first-arrival traveltimes. Figure 1 shows different time slices from the OBS data; the dark-blue areas indicate no data zones. Some areas within the block have no data, possibly because of production infrastructure at those sites. Sail-lines have to curve around those areas.

Picking in Polar Coordinates

First-arrival wavefronts are circular in the near-offsets and quickly deform into irregular shapes with complex patterns in far-offsets (see the time-slices in Figure 1). Such patterns can be optimally parameterized in 2D polar coordinate system, where the source geographical position is at the center of the system. In such a coordinate system a circular wavefront can be picked using a single pick as is the case in Figure 1(a). As the wavefronts deform gradually with time as in Figure 1(b), (c), and (d) more picks are needed.

The decision of how many picks are needed to fully represent a wavefront is based on real-time interpolation during the picking process. An interactive application, using a graphical user interface (GUI), uses a pointer position to compute the wavefront before making the pick by clicking the mouse. Therefore, the interpreter (user) can optimize the number of picks by moving the pointer as far as possible from the last pick, as long as the interpolated picks follow the tracked wavefront. The following equations are used in real-time to interpolate between the closest pick and the current pointer position as a function of azimuth θ:

$$\begin{aligned} r(\theta) &= r_{\text{pick}} + \frac{(r_{\text{pointer}} - r_{\text{pick}})}{(\theta_{\text{pointer}} - \theta_{\text{pick}})} * (\theta - \theta_{\text{pick}}), && (1) \\ x &= x_{\text{src}} + r(\theta) * \sin(\theta), && (2) \\ y &= y_{\text{src}} + r(\theta) * \cos(\theta), && (3) \end{aligned}$$

where x and y are the coordinates of the interpolated point, x_{src} and y_{src} are the source coordinates, $(r_{\text{pointer}}, \theta_{\text{pointer}})$ are the polar coordinates of the moving pointer, and $(r_{\text{pick}}, \theta_{\text{pick}})$ are the polar coordinates of the closest pick.

The picks are registered with geographical coordinates, and therefore they bear no relation to acquisition geometry. Therefore, this method does not suffer from the irregularity of the data.

Picking Time-Slice Sampling

As mentioned above, the goal of the traveltime picking is to generate a starting model for multiscale FWI. The bandwidth of the first FWI run governs the time-slice interval used for picking. To avoid cycle-skipping, data calculated from the initial model has to be within half a period of the observed data. To meet this criterion, we choose a time-slice interval of half the period of the dominant frequency of the first iteration of FWI. For the OBS data, FWI is applied to 4 Hz data, and therefore the time-slice interval should be less than 125 milliseconds. We selected time slices at 100 ms intervals for the GOM study.

Quality Control

Consistency of traveltime picking is crucial for computing a high-quality tomogram. Therefore, we developed a QC tool to monitor the relationship between picks from different gathers. Figure 2 shows QC-plots for different azimuth angles for the time-slice 2.0 seconds. In each plot, a color-coded block is plotted on-top of each source position, the color-coding represents the distance from the source location to the first-arrival wavefront at a given azimuth (below the QC-panel in figure 2). If a pick in a given gather does not follow the areal trend, the picking for that gather is reviewed and adjusted to follow the trend. This exercise is repeated for every picked time-slice.

Inversion using Pseudo-Receivers

The picking and QC-ing procedure described above will result in a set of continuous contours for each shot, where the contours represent the first-arrival distance from the source point at a fixed traveltime. In preparation for ray tomography, the continuous contours are sampled uniformly azimuthally, and each sample used as a pseudo-receiver with the first-arrival traveltime as the one for the sampled contour. This leads to a pseudo-receiver-geometry. For the OBS data, the traveltime-contours are sample 360 with equal angular spacing, and the associated traveltimes are used in traveltime tomography as discussed in the following section.

TOMOGRAPHY

To compute the tomogram, we find the slowness model that minimizes the objective function

$$f(\mathbf{s}) = \frac{1}{2} \sum_{i=0}^{N_t} \left(w_i \delta\tau_i(\mathbf{s})\right)^2, \tag{4}$$

where $\delta\tau_i$ is the difference between the observed and calculated traveltime, w_i is a positive weighting factor, N_t is the number of data samples included in the inversion, and $\mathbf{s}$ is the slowness model. Traveltime picks at far-offsets are subject to higher uncertainty due to the low-amplitude of the diving waves. The far-offsets often dominate the residual, and the inversion will have low sensitivity to traveltime errors with near offsets. To balance the inversion, we use the weighting factor

$$w_i = \frac{1}{\tau_{\text{obs}}^p}, \tag{5}$$

where τ_{obs} is the observed traveltimes, and p is a positive power parameter chosen empirically; the higher the parameter p, the more biased the inversion toward near-offset picks (we choose $p = 0.5$). The objective function is

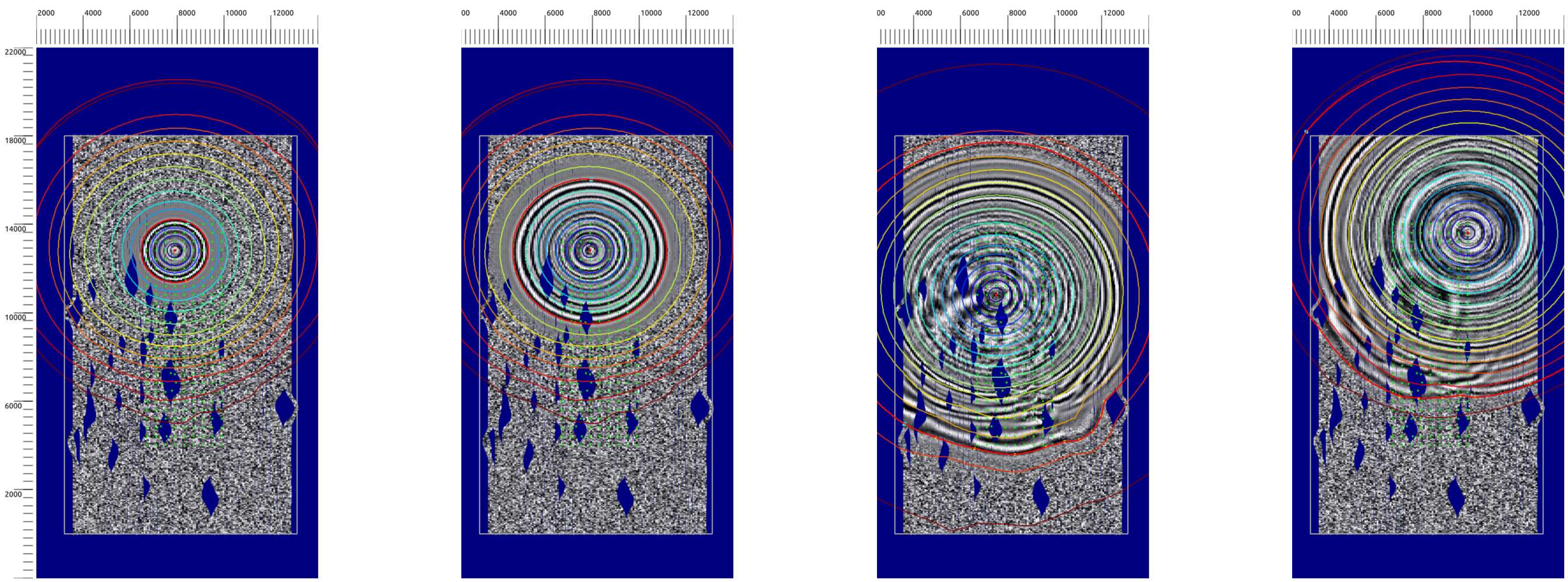

(a) 0.8 seconds
1 pick

(b) 1.6 seconds
2 picks

(b) 2.8 seconds
14 picks

(d) 3.2 seconds
9 picks

Figure 1: Different time slices with their picks (yellow dots, and red interpolated polygon). The colored contours are wavefront polygons from other time slices. The green dots are shot locations, and the red dot represents the viewed shot-gather. Gray scale images represent the recorded waveform at the active time slice. No data coverage zones are indicated by the dark blue color. The vertical and horizontal distances are on a scale of meters. Picks outside the data coverage are discarded before tomography.

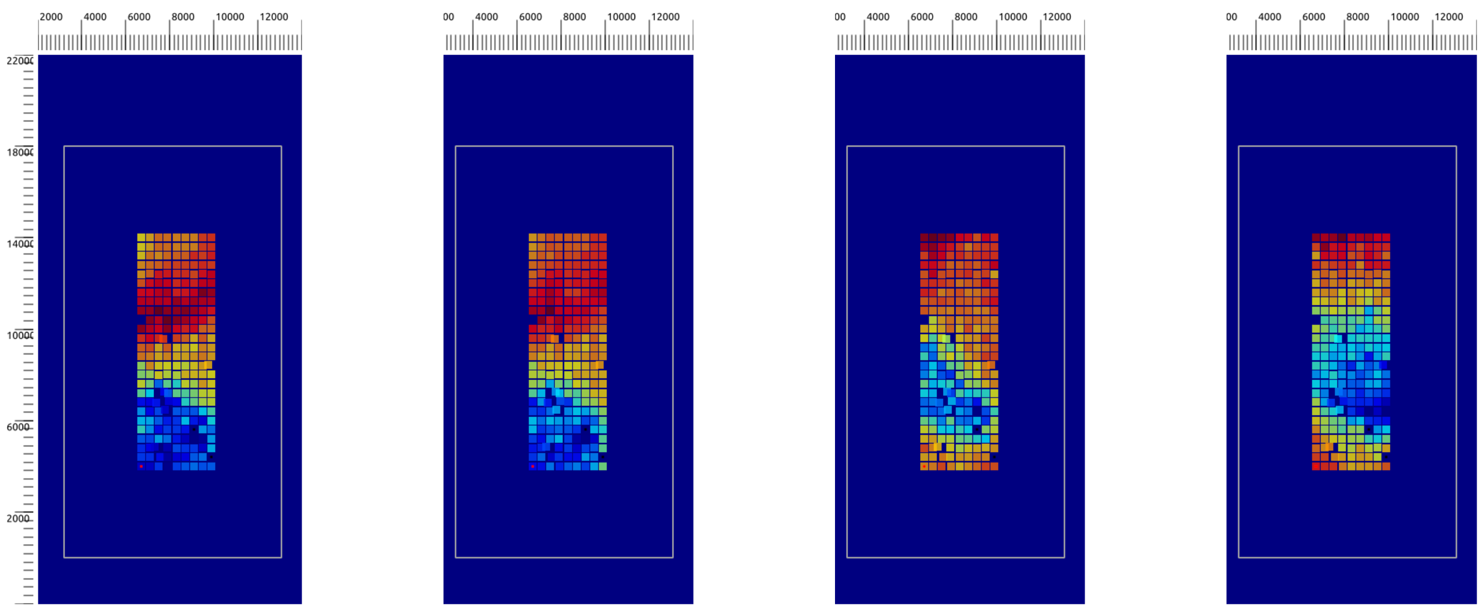

(a) 0°

(b) 45°

(c) 135°

(d) 225°

Figure 2: Panels for QC-ing azimuth-dependent distance for the 2 sec time-slice. The colors represent the distribution of the radial distance from the source-point to the first-arrival wavefront at the corresponding azimuth. This tool is used to detect anomalous picks that does not follow the trend of surrounding gathers.

minimized by iteratively solving the following reweighted preconditioned linearized system of equations for the slowness update $\delta\mathbf{s}$:

$$\mathbf{WJPy} = \mathbf{W}\delta\tau, \qquad (6)$$
$$\delta\mathbf{s} = \mathbf{Py}, \qquad (7)$$

where $\mathbf{W}$ is a diagonal matrix where $\mathbf{W}_{ii} = w_i$, $\mathbf{WJ}$ is the Jacobian matrix for the objective function in equation 4, $\mathbf{P}$ is a preconditioning operator where the adjoint $\mathbf{P}^\dagger$ is the Gaussian smoothing operator, and $\mathbf{y}$ is a temporary vector. At every nonlinear iteration, the slowness update is solved for using the Gauss-Newton method

$$(\mathbf{WJP})^\dagger \mathbf{WJPy} = (\mathbf{WJP})^\dagger \mathbf{W}\delta\tau, \qquad (8)$$
$$\delta\mathbf{s} = \mathbf{Py}. \qquad (9)$$

This least-squares inversion is solved using only a few iterations (two iterations in for the OBS data). The role of the preconditioner $\mathbf{P}$ is to insure that the updates are very smooth; at early iterations the Gaussian function is chosen to span the whole model, and the width is gradually reduced to 800 meters, which is twice the distance between the OBS stations to avoid aliasing. The height of the Gaussian filter is 15% of its width.

The golden-section method is used to calculate the steplength α after computing the step direction $\delta\mathbf{s}$. After that, the slowness model is updated using $\mathbf{s}_{k+1} = \mathbf{s}_k + \alpha\delta\mathbf{s}$.

FINAL RESULTS

Figure 3 shows the final tomogram calculated from the traveltimes picked from time slices. The velocity gradually increases with depth, and there is a velocity inversion at the depth of 1 km. A gentle anticlinal structure is prominent in the middle of the volume. Figure 4 shows the ray density associated with the tomogram in Figure 3. Usually, ray-density diagrams show high ray-count around the refractor. As can be seen from Figure 4, there is one shallow refractor (depth ∼500 m) and a deep one at 1.5 km depth.

The primary objective of picking first-arrivals and tomography is to compute a starting velocity model, where the calculated waveforms are not cycle-skipped relative to the observed waveforms. Figure 5 show the 0-5 Hz observed and the calculated waveform using the final tomogram. Significant deflections are prominent in the data, possibly due to slow shallow anomalies. However, the calculated waveforms are in-phase with the observed data, matching even the strong deflections in the events. This indicates readiness to apply FWI to the data, which is my next task.

CONCLUSION

We present an efficient method for picking first-arrival traveltimes for data with dense wavefield sampling. This method allows for picking geographically on time slices as opposed to the traditional picking of times in CSGs or common offset gathers. The picks are interpolated in polar coordinates to minimize the number of picks needed to characterize areally curved wavefronts.

The method is applied to 3D OBS data, and the traveltime picks are used in tomography to generate a tomogram. These tomograms predict first-arrivals that are inphase with the observed first-arrival data. The estimated saving in picking time is about 80% compared to manual picking of traveltimes from trace to trace.

REFERENCES

Symes, W., and J. Carazzone, 1991, Velocity inversion by differential semblance optimization: Geophysics, **56**, 654–663.

Tarantola, A., 1984, Inversion of seismic reflection data in the acoustic approximation: Geophysics, **49**, 1259–1266.

Virieux, J., and S. Operto, 2009, An overview of full-waveform inversion in exploration geophysics: Geophysics, **74**, WCC1–WCC26.

Woodward, M., D. Nichols, O. Zdraveva, P. Whitfield, and T. Johns, 2008, A decade of tomography: Geophysics, **73**, VE5–VE11.

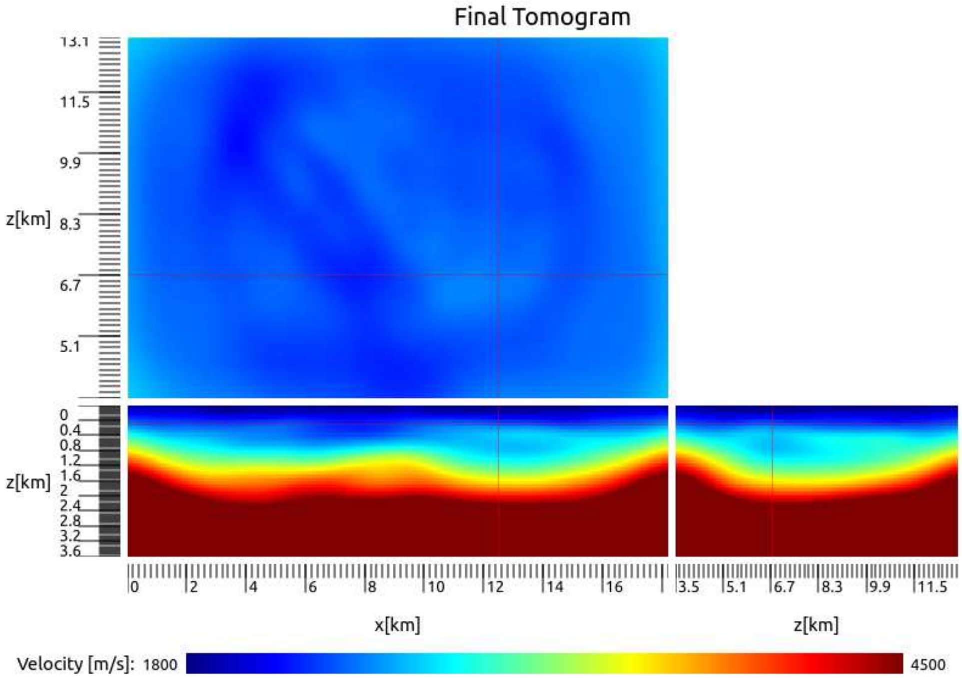

Figure 3: The final tomogram after 50 iterations: the top-panel is a depth slice, the lower-left panel is an inline-slice, and lower-right panel is a crossline slice inside the tomogram. The positions of the slices are highlighted by the vertical and horizontal red lines.

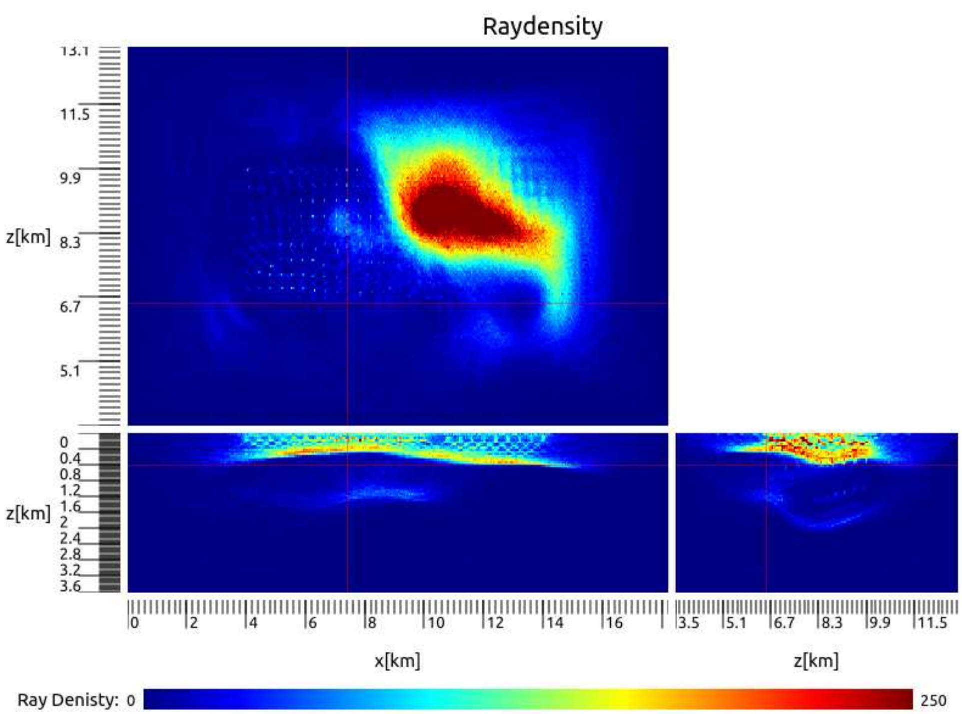

Figure 4: Ray density for the final tomogram.

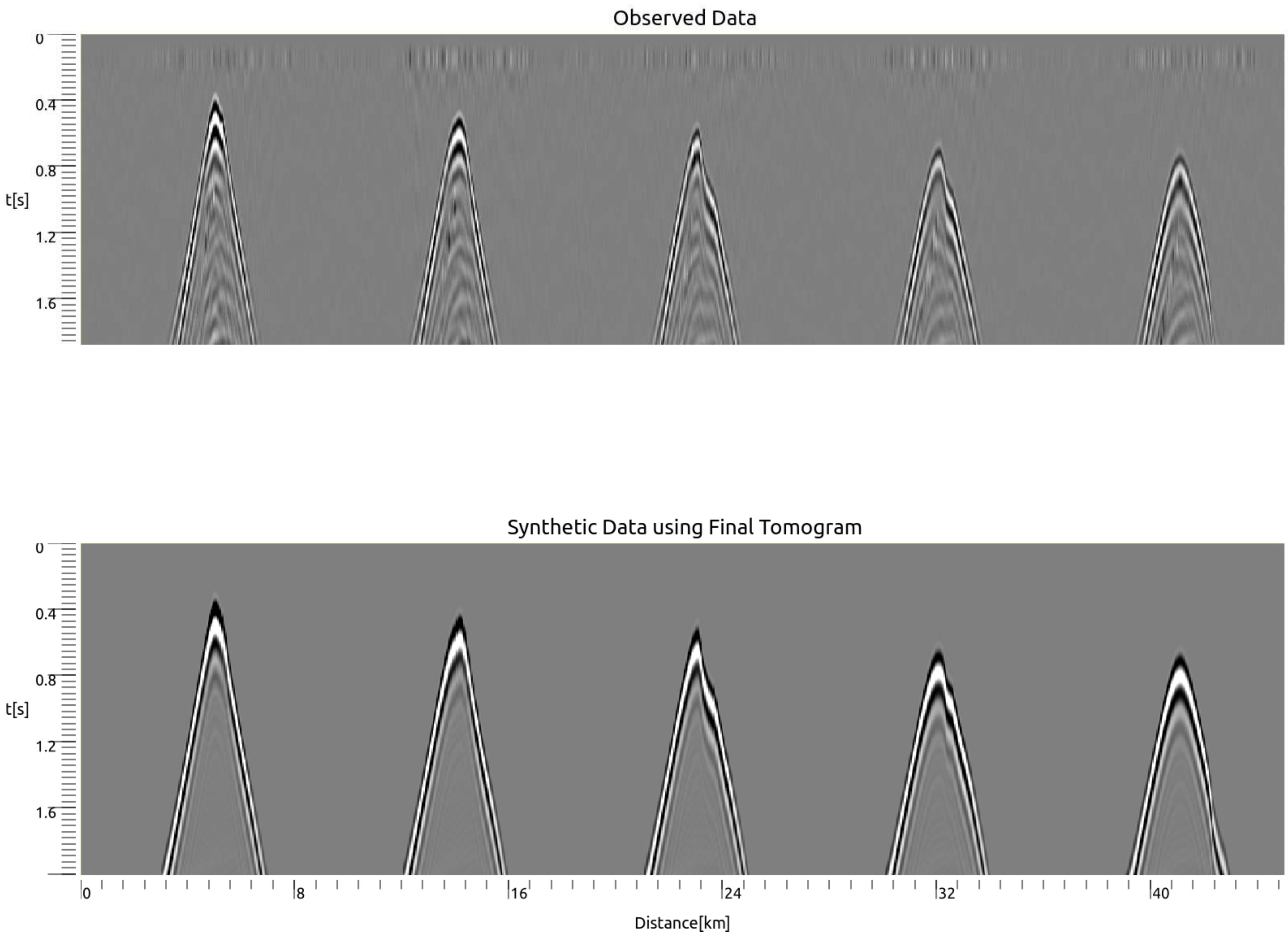

Figure 5: The observed data (top) and the calculated data using the final tomogram (bottom).